Int. J. Electrochem. Sci., 10 **(2015)** 1966 - 1978

International Journal of ELECTROCHEMICAL SCIENCE
www.electrochemsci.org

Assessment of Dimethylbenzodiimidazole as Corrosion Inhibitor of Austenitic Stainless Steel Grade 316L in Acid Medium

C. Cardona[1], A. A. Torres[2], J.M. Miranda-Vidales[3], J.T. Pérez[2], M. M. González-Chávez[4], H. Herrera-Hernández[5], L. Narváez[6,]*

[1]Universidad Tecnológica de Querétaro, Pie de la Cuesta 2501, C.P. 76148. Querétaro, Qro. México.
[2]Instituto Mexicano del Transporte, Km 12 Carretera Qro-Galindo, C.P. 76700. Querétaro, México.
[3]Instituto de Metalurgia, Universidad Autónoma de San Luis Potosí, Sierra Leona 550, Lomas 2ª. Sección, C.P. 78210. San Luis Potosí, SLP, México.
[4]Facultad de Ciencias Químicas, Universidad Autónoma de San Luis Potosí, Av. Dr. Manuel Nava 6, C.P. 78210. San Luis Potosí, SLP, México.
[5]IIN Applied Research and Surface Corrosion Engineering, Universidad Autónoma del Estado de México, Blvd. Universitario s/n, Predio San Javier Atizapán de Zaragoza, C.P. 54500. Edo. de México, México.
[6]Facultad del Hábitat, Universidad Autónoma de San Luis Potosí, Niño Artillero 150, C.P. 78290. San Luis Potosí, SLP, México.
[*]E-mail: narvaezl@uaslp.mx

Received: 1 May 2014 / *Accepted:* 19 November 2014 / *Published:* 19 January 2015

In this research the performance of an imidazole derivative [Dimethylbenzodiimidazole (2,7-dimethyl-3,6-dihydrobenzo[1,2-d;3,4-d'] diimidazole)] (BDI) as organic inhibitor to minimize pitting corrosion of 316L Stainless Steel in sulphuric acid solution at room temperature was evaluated by means of electrochemical measurements. The inhibitor concentrations studied in the system steel/acid were 0, 10, 20, 40, 60, 80, 100 and 120 ppm. Electrochemical techniques as polarization curves and electrochemical impedance spectroscopy (EIS) were employed to evaluate the inhibitor behavior. The results of polarization curves showed that BDI causes a shift at the corrosion potential to more positive values, and a decrease in the corrosion current, indicating that the inhibitor restricts the anodic metal dissolution reaction, so, the inhibitor was classified into anodic type. Whereas, the impedance spectra (e.g. Nyquist plots) showed a continuous increase of the diameter of semicircle, which is associated to the charge transfer resistance (R_{ct}) as a function of increasing inhibitor concentration, this behavior follows the mechanism of physical adsorption of the molecule leading to the formation of a protective barrier layer on steel surface. Also, it was found that the greatest corrosion inhibiting efficiency (IE) was attained at 40 ppm. This is sufficient reason to consider that the organic compound BDI is a good alternative as corrosion inhibitor for 316L Stainless Steel in acid medium.

Keywords: Pitting Corrosion, Sulfuric Acid, Inhibitor, Dimethylbenzodiimidazole, 316L Stainless Steel, Electrochemical Impedance Spectroscopy, Organic Molecules.

1. INTRODUCTION

Austenitic stainless steel is the material commonly used in a wide variety of applications in industry because of relatively low cost. They contain between 16 to 18% chromium and about 12% nickel, which contribute to their good mechanical strength and excellent corrosion resistance. Besides, it is worth noting their hygienic and aesthetic qualities [1,2]. In view of these desirable properties, stainless steels have been used as an alternative material to the construction and installation of nuclear reactors & thermal power plants, equipment for food and pharmaceutical industry, drinking water treatment systems and wastewater, as well as chemical plants, aeronautics, pipes for transport oil & gas, etc., given the characteristics that distinguish them [3,4]. However, when stainless steel is transformed into wire or pipe, it is necessary to submit it to a heat treatment (e.g. annealing) in order to relief the structure from the residual stress [5]. During annealing a thin oxide layer of chromium depleted grows on the SS316-L base metal, it is known as scale layer and is composed by $Fe^{+2}O^{-2}$. These oxide layers may be removed by mechanical processes, or by means of chemical attack such as striping, thereby providing a good finish (gloss, texture, and resistance to oxidation of the material). [6,7]. The striping is a part of final production process of some steel products and is usually done with acid mixtures, where the type of acid used is important as they have a strong influence on the quality of surface finish. One of the common mixtures is usually performed with hydrofluoric acid (HF) and nitric acid (HNO_3). Despite its-efficiency, the use of HNO_3 causes serious atmosphere damage such as nitrogen oxide (NO_x) emissions that are highly polluting [8]. Research is under way to replace HNO_3 with some mixtures of hydrochloric acid (HCl) or sulfuric acid (H_2SO_4). The advantage of using nitric acid-free mixtures is the removal of the NO_X emitted into the environment, for they are an important contamination factor [5-8]. However, all pickling mixtures containing aggressive acids which in contact with the metal surface causes important loss of the material, this results in the formation of pits by metal ion dissolution (Me^+) from the material as a consequence of a electrochemical reactions (anodic and cathodic).

The decrease of metal dissolution during the contact with the acid mixtures can be achieved in a practical and economical way by using corrosion inhibitors. Any corrosion inhibitor can be defined as a substance or combination of substances in a suitable concentration to avoid or reduce the electrochemical reactions (corrosion damage) of a material during its exposure to aggressive environments [9-11]. The corrosion inhibition mechanism by using organic compounds is often related to their adsorption on the metal surface. Adsorption of inhibitors depends on the physicochemical properties of functional groups, steric factors, aromaticity and the electronic structure of the inhibitor [12]. The majority of inhibitors used in acid medium are organic compounds containing electronegative functional groups, π-electrons and heteroatoms such as Nitrogen (N), Oxygen (O), Phosphorus (P), Sulphur (S), triple bonds and aromatic rings [13-20].

Previous studies have reported that imidazoles and their derivatives are effective inhibitors, which possess two nitrogen atoms in a heterocyclic ring favoring the anchoring of the molecule on the metal surface [21]. The inhibition efficiency of organic compounds of the imidazole derivatives has

been studied in several works on stainless steels in acid medium. Compounds such as N-vinylimidazoles, 2-Mercaptobenzimidazole, 4-substitud pyrazoles-5 ones, 1,2,3-benzotriazoles and 4-phenylthiazole have proved that compounds with not shared pair electrons in the atoms of nitrogen can be absorbed on the steel surface forming a protective film [4, 22-25]. However, despite the number of investigations on the effects of inhibition of organic nitrogen compounds on stainless steel [22,23,26,27], it is important to have more information about the mechanism of adsorption of these molecules and the inhibition efficiency. This work proposed the study of Dimethylbenzodiimidazole (2,7-dimethyl-3,6-dihydrobenzo [1,2-d;3,4-d´]di-imidazole) (BDI) as corrosion inhibitor for stainless steel in acid medium, beside the inhibition efficiency of this compound and the feasibility of its use in a stripping mixture of H_2SO_4 are discussed. One of the most important contributions of this research is the use of a type of Benzimidazole compound that has not previously been used as a corrosion inhibitor in Stainless Steels in sulphuric acid. This compound has been prepared in the Organic Synthesis Laboratory in Chemical Faculty at the University of San Luis Potosi, Mexico [28].

2. EXPERIMENTAL DEVELOPMENT

2.1. Materials

The corrosion inhibition test was performed in an austenitic Stainless Steel (SS) AISI 316L with a chemical composition as that given in Table 1. Steel plates of 3 cm × 2 cm × 0.2 cm were prepared in duplicate, in order to be used as working electrodes (WE) in electrochemical testing.

Table 1. Chemical composition of austenitic stainless steel (AISI 316L) in weight %.

C	Si	Mn	P	S	Cr	Cu	N	Ni	Mo	Fe
0.017	0.37	0.89	0.027	0.001	18.86	0.32	0.044	10.25	2.0	Balance

Prior to the electrochemical experiments, the samples were mechanically polished according to conventional metallographic preparation. The working surface was previously rinsed with distilled water, degreased in acetone and then dried in warn air before each test.

2,7-dimethyl-3,6-dihydrobenzo[1,2-d;3,4-d’] diimidazole compound (referred as BDI) was used as inhibitor at different concentrations, the molecular structure of this compound is shown in Figure 1. This tricyclic compound has two imidazole rings bonded to a benzene ring. Seven concentrations of BDI were tested: 10 ppm, 20 ppm, 40 ppm, 60 ppm, 80 ppm, 100 ppm and 120 ppm. A mixture of 0.5 M of H_2S0_4 with the different concentrations of the inhibitor was used as electrolyte. The temperature was maintained at 25 °C during all experiments. A steel plate without inhibitor was evaluated as control, which was designated as reference material (blank). Distilled water was used to prepare the solutions, and all chemicals used were reagent-grade. Fresh solutions were prepared for each experiment.

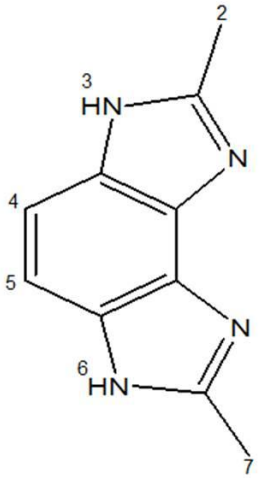

Figure 1. Molecular structure of Dimethylbenzodiimidazole (2,7-dimethyl-3,6-dihydrobenzo [1,2-d; 3,4-d'] diimidazole) BDI [28].

2.2 Electrochemical measurements

Electrochemical tests were performed using a potentiostat Gamry DHC2 model, coupled to a computer with Echem Analyst software for collecting the experimental data. An arrangement of three electrodes were used according to the ASTM G3, ASTM G5, ASTM G59 standards; saturated calomel electrode (SCE) as reference electrode; graphite rod as a counter electrode and samples of 316L SS as working electrode [29-31]. The exposed area was 1 cm^2. All tests have been performed at 25°C in nondeaerated solutions under unstirred conditions.

Polarization curves. The test conditions of the polarization curves were obtained on a scanning range of -700 mV to 1200 mV with respect to the open circuit potential (OCP), at a scan rate of 2.5 mV s^{-1} [31]. Before each test, the working electrode was immersed in test electrolyte during 30 min to allow adsorption of the inhibitor on the metal surface. The experiments were conducted after this 30 min exposure on the test solution, when the open circuit potential had reached a steady-state condition. The corrosion rate in terms of current density (i_{corr}) and corrosion potential (E_{corr}) were determined by the intersection of the extrapolating anodic and cathodic Tafel slopes.

Electrochemical Impedance Spectroscopy (EIS). Electrochemical impedance measurements were performed in a frequency range of 55 KHz to 10 mHz with an amplitude signal of ±10 mV around E_{corr} [29,32]. Before each test, the working electrode was immersed in test electrolyte during 30 min to allow adsorption of the inhibitor on the metal surface. The experiments were conducted after this 30 min exposure on the test solution, when the open circuit potential had reached a steady-state condition. The EIS data obtained were described using Nyquist plots and Bode diagrams in order to determine the electrochemical parameters. An appropriate equivalent electric circuit (ECC) was proposed in order to fit the experimental data points with the electrical model for computing the key parameters, such as electrolyte resistance (R_s) and the charge-transfer resistance (R_{ct}). In the model a CPE is used in place of a capacitor due to compensate for non-homogeneity.

3. RESULTS AND DISCUSSION

3.1. Tafel extrapolation curves

The inhibition efficiency (*IE*) was obtained from the polarization curves, which was determined by Tafel slopes extrapolation. The inhibition efficiency *IE* (%) values were obtained using the Equation 1 [33, 34]:

$$IE(\%) = 100\left[\frac{i_{corr} - i^{0}_{corr}}{i_{corr}}\right] \quad (1)$$

where i°_{corr} and i_{corr} are the corrosion current density values in the absence and presence of the inhibitor for stainless steel samples exposed to 0.5 M H_2SO_4, respectively.

The inhibition efficiency *IE (*%) can also be calculated from the data of Electrochemical Impedance Spectroscopy (EIS) through the use of Equation 2 [27,34]:

$$IE(\%) = 100\left[\frac{R_{ct} - R^{0}_{ct}}{R_{ct}}\right] \quad (2)$$

where R°_{ct} and R_{ct} are charge transfer resistance values in the absence and presence of the inhibitor, respectively, which is similar to the Equation 1. $1/R_{ct}$ usually indicates the corrosion rate.

The current density i_{corr} was calculated from Equation 3 [31,35]:

$$i_{corr} = \frac{\beta}{R_p} \quad (3)$$

where i_{corr} is the corrosion current density related to the polarization resistance R_p and β is the Stern-Geary coefficient.

The corrosion rate for each inhibitor concentration was determined according to Equation 4 [33]:

$$CR = K\,\frac{i_{corr}\,W}{nD} \quad (4)$$

where *CR* is the corrosion rate in mm/yr, *K* is equal to 3.27 x 10^{-3} mm g/μA cm yr, i_{corr} is the corrosion current density at μAcm^{-2}, *W* is the atomic weight of the element, *n* is the number of electrons required to oxidize an atom of the element in the corrosion process, and *D* is the density in g cm^{-3} in 316L stainless steel is 7.98 [36].

Figure 2 shows the polarization curves obtained from 316L SS in a 0.5M solution of H_2SO_4. The concentrations used were 10 ppm, 20 ppm, and 40 ppm. The curves were obtained after 30 min of immersion and then the test was performed.

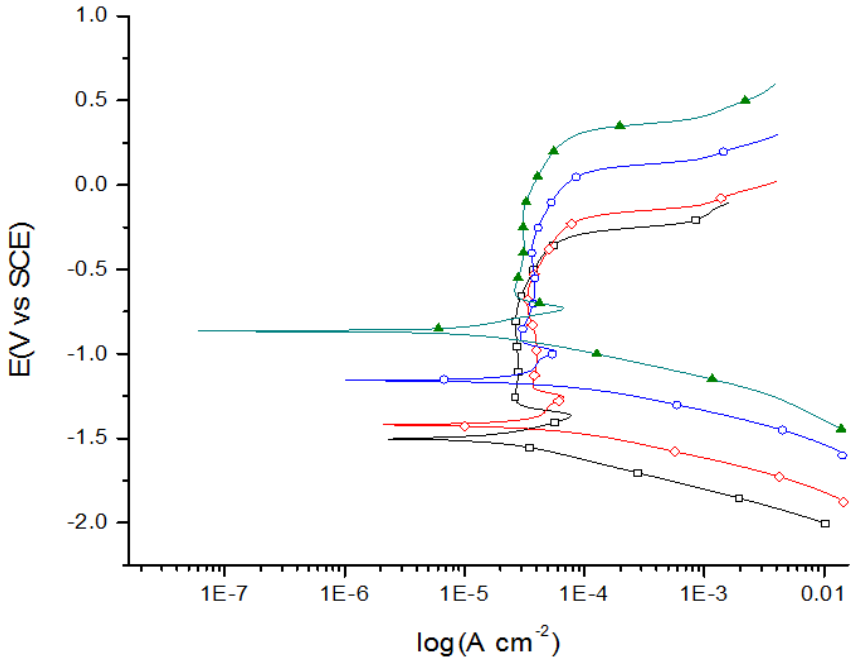

Figure 2. Polarization curves obtained from 316L SS in 0.5M of H_2SO_4 containing the inhibitor at: (◊) 10 ppm; (○) 20 ppm; (▲) 40 ppm and (□) without inhibitor (blank) after 30 min of immersion in the mixture at 25°C.

Figure 3 shows the polarization curves obtained for 316L SS in a 0.5M solution of H_2SO_4 using BDI concentrations of 60 ppm, 80 ppm, 100 ppm and 120 ppm after an immersion time of 30 min in order to carry out the testing procedure immediately after the immersion.

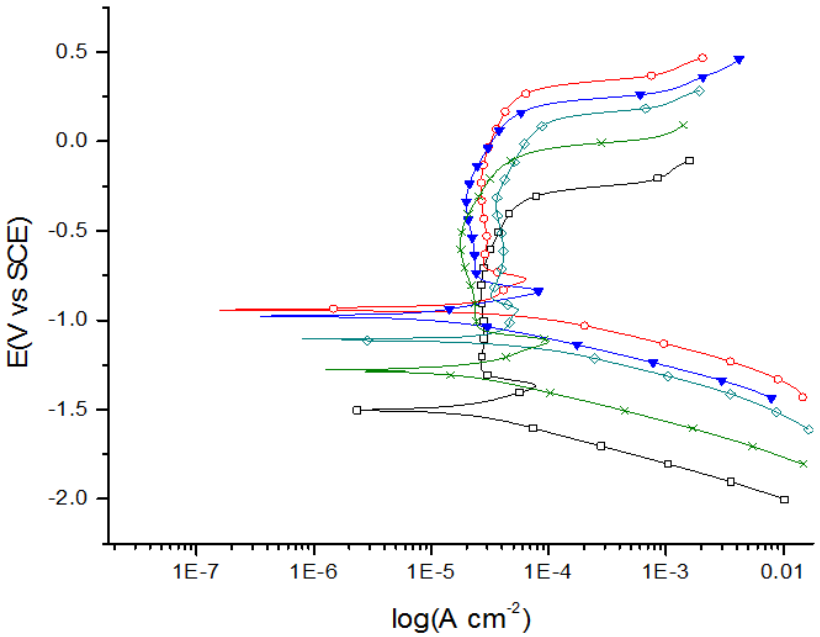

Figure 3. Polarization curves obtained from 316L SS in 0.5M H_2SO_4 containing the inhibitor at: (○) 60 ppm, (▼) 80 ppm, (◊) 100 ppm, (X) 120 ppm and (□) without inhibitor (blank) after 30 min of immersion in the mixture at 25°C.

In Figures 2 and 3 it can be observed that the 316L SS dissolution shows Tafel behavior. In general, the dissolution of the SS decreased as the inhibitor concentration increased. Thus, when the inhibitor was added, it causes a shift on the corrosion potential, E_{corr}, to nobler values with respect to the blank. This indicates the anodic nature of the inhibitor [37,38]. The addition of the inhibitor causes a slight decrease in the current density and presents two trends: By increasing the inhibitor content (since 10 ppm to 40 ppm), the corrosion potential value is shifted to more positive values, showing value a 0.622 V of ΔE with respect to the blank (Figure 2). The relative density current decreases and the efficiency increases. However, in Figure 3, when increasing the concentration from 60 ppm to 120 ppm, the current density increased too, generating negative values of corrosion potential thus the inhibitor efficiency diminishes. This behavior could be explained by the geometrical structure and length of the compound chain. According to Figure 1, BDI shows a large chain in its structure in comparison to the imidazole compound. Is common on a very large molecule like BDI that tends to twisted or bend over itself in the entire space as the inhibitor concentration increases, thus forming loops that avoid the adsorption of the inhibitor on the metal surface. By this way the bonding energy of the system depends on the distance between organic molecules and the metal surface [21]. At large distance the energy is zero, there is not interaction. While at distances of several atomic diameters attractive forces dominate the adsorption mechanism.

The electrochemical parameters (E_{corr}, i_{corr} and IE%) obtained from the polarization curves for 316L SS in 0.5M H_2SO_4 in the absence and presence of inhibitor concentration during 30 minutes of exposure, are shown in Table 2.

Table 2. Electrochemical parameters and inhibition efficiency percentage of the BDI 316L SS in 0.5M of H_2SO_4, with and without inhibitor, after 30 min of immersion in the mixture at 25 °C.

Concentration ppm	$E_{corr\ (SCE)}$ (V)	i_{corr} ($\mu A/cm^2$)	IE %
Blank	-1.255	38.336	-
10	-1.185	29.679	22.6
20	-0.918	18.706	51.2
40	-0.622	8.808	77.0
60	-0.708	11.449	70.1
80	-0.732	14.826	61.3
100	-0.868	18.759	51.1
120	-1.038	25.410	33.7

In Table 2 could be observed the displacement of the corrosion potential by more than 600 mV in the positive direction and decrease in the corrosion current densities, from 0 to 40 ppm indicate that presence of BDI in corrosion medium retards the development of aggressive conditions and reduces the dissolution of SS. But when the inhibitor concentration increases from 60 to 120 ppm, the corrosion potential, E_{corr}, decreased 400 mV towards negative values. Therefore, BDI is a good passivator at lower concentrations and does not passivate at higher concentrations according to as explained above. At higher concentrations BDI molecules are not able to form a resistive layer

whereas at lower concentrations the resistive layer may be formed with the help of ions like $(HSO_4)^{-1}$ and $(SO_4)^{2-}$ present in the solution. According to the results obtained, is possible, suggest that the optimal inhibitor concentration is 40 ppm at 25 °C due to this it is possible to achieve an inhibitory efficiency of 77%.

The following equations represent the reaction of the metal in acid solutions: equation 5 shows the metal dissolution and equations 6 and 7 indicate the cathodic reactions that could be derived from oxidizing agents [16, 39].

Anodic reaction:

$$Fe \longrightarrow Fe^{2+} + 2e^- \quad (5)$$

Cathodic reactions:

$$2H^+ + 2e^- \longrightarrow H_2 \quad (6)$$

$$½O_2 + 2H^+ + 2e^- \longrightarrow H_2O \quad (7)$$

While the adsorption mechanism of the organic inhibitor at the interface electrode/electrolyte can take place through a displacement process of adsorbed water molecules at the inner Helmholtz plane of the electrode, likely in agreement with the following reaction.

$$Org_{(aq)} + mH_2O_{(ads)} \longrightarrow Org_{(ads)} + mH_2O_{(aq)} \quad (8)$$

3.2 Electrochemical Impedance Spectroscopy (EIS)

In Figures 4 and 5 show the EIS results through Nyquist and Bode diagrams of 316L SS in 0.5M H_2SO_4 solution in absence and presence of inhibitor at several concentrations. In Figure 4, it can be observed that the semicircle diameter becomes larger when the BDI concentration is increased at 10, 20 and 40 ppm, which indicates that the inhibitor increases the resistance to charge transfer, R_{ct}. This behavior may be associated to a molecular adsorption mechanism of the organic compound referred as BDI over the polished metal surface, thus forming a multilayered assembly that prevents the adsorption of SO_4^- ions (which is responsible of pitting corrosion process on metals).

The occurrence of two time constants observed in Figure 5b, suggests the presence of two different processes during the perturbation; one is related to a mechanism of molecular adsorption of inhibitor onto the metal surface, and the second one is a constant related to the electrochemical interactive forces of the double electrochemical layer operating in the electrolytic system and species corroded. This second time constant that operates at intermediate frequencies can be interpreted as a resistance to charge transfer, R_{ct}. On the other hand, figure 5a (log Z vs log f) shows that the impedance values increase as the inhibitor concentration also increases. This is also related to charge transfer resistance, R_{ct}.

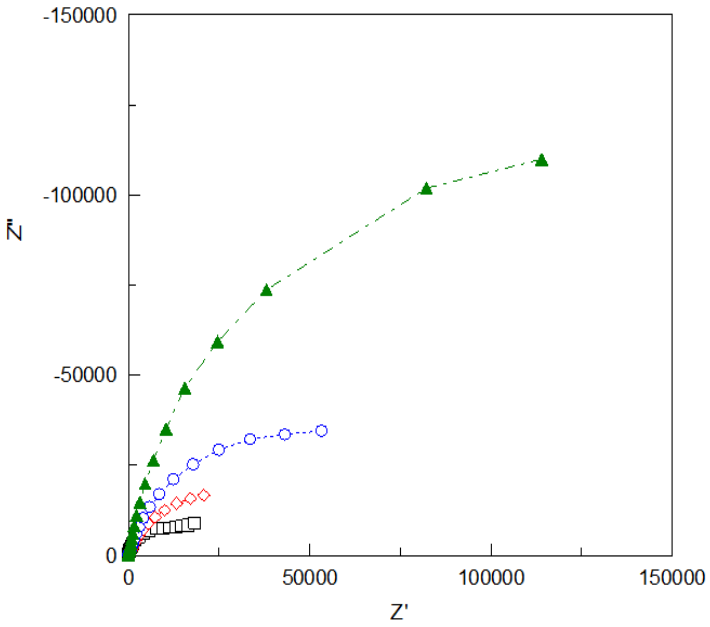

Figure 4. Nyquist diagram obtained from 316L SS in 0.5M of H_2SO_4 containing the inhibitor at: (◊) 10 ppm; (○) 20 ppm; (▲) 40 ppm and (□) without inhibitor (blank) after 30 min of immersion in the mixture at 25°C.

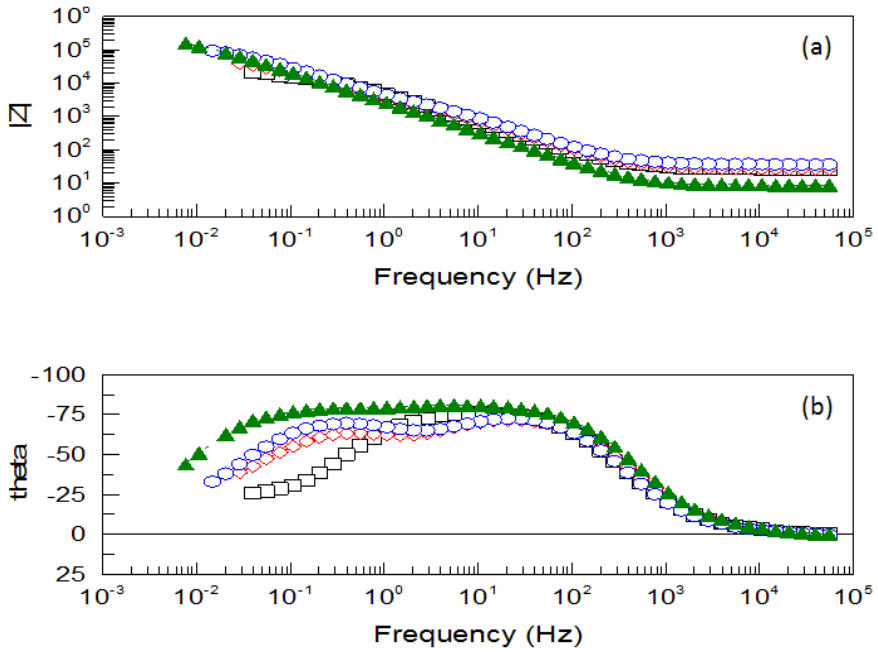

Figure 5. Bode plot obtained from 316L SS in 0.5M of H_2SO_4 containing the inhibitor at: (◊) 10 ppm; (○) 20 ppm; (▲) 40 ppm and (□) without inhibitor (blank) after 30 min of immersion in the mixture at 25°C.

Figures 6 and 7 show the EIS data in the representation of Nyquist and Bode diagrams of 316L SS in 0.5 M of H_2SO_4 solution in absence and presence of various concentrations of the inhibitor. Figure 6 shows that when the concentration increases from 60 ppm to 80 ppm, 100 ppm or 120 ppm,

the semicircles diameters decrease. This may indicate a poor adsorption of the inhibitor on the metal surface due to the structural geometry of organic compound (BDI).

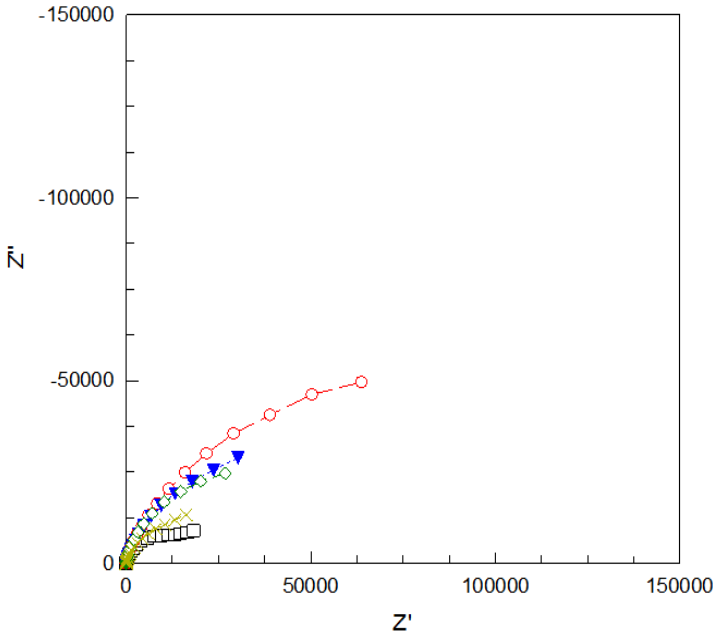

Figure 6. Nyquist diagram obtained from 316L SS in 0.5M of H_2SO_4 containing the inhibitor at: (○) 60 ppm, (▼) 80 ppm, (◊) 100 ppm, (X) 120 ppm and (□) without (blank) inhibitor after 30 min of immersion in the mixture at 25°C.

Figure 7a shows that as the concentration of inhibitor increases the impedance decreases. This may be due to the inhibitor molecules that stop adhering to the metal surface. In Figure 7b two coupled processes that could be represented by two time constants are shown.

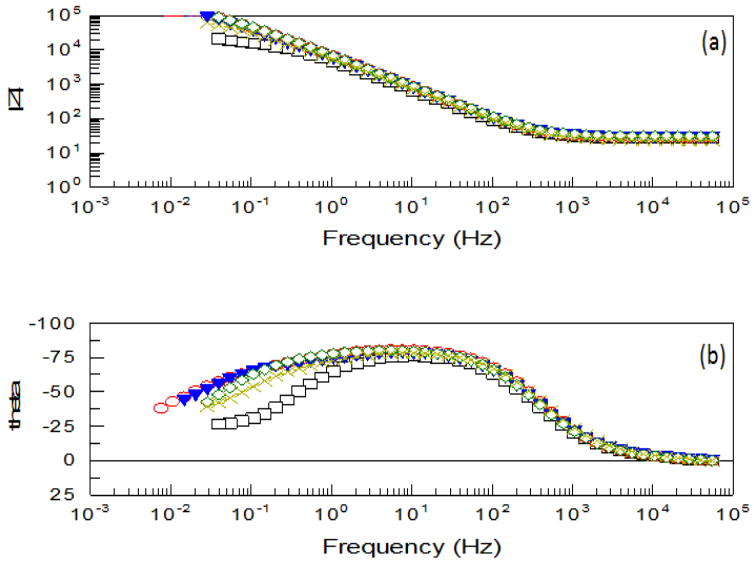

Figure 7. Bode plot obtained from 316L SS in 0.5M of H_2SO_4 containing the inhibitor at: (○) 60 ppm, (▼) 80 ppm, (◊) 100 ppm, (X) 120 ppm and (□) without inhibitor (blank) after 30 min of immersion in the mixture at 25°C.

The results described above can be interpreted in terms of the RC equivalent electrical circuit shown in Figure 8. This circuit model was used to characterize the system that contained from 10 to 120 ppm BDI, which is composed by two constant phase elements (CPE) with their respective resistors, R_{mol} (organic molecules resistance) and R_{ct} (charge transfer resistance), connected in parallel and its solution resistance (R_s) that is connected in series; this circuit arrangement is due to the presence of two interfaces in the system H_2SO_4 + inhibitor/metal; one describes the process related to the organic molecules adsorption onto metal surface and the other the characteristics of the electrical double layer interface.

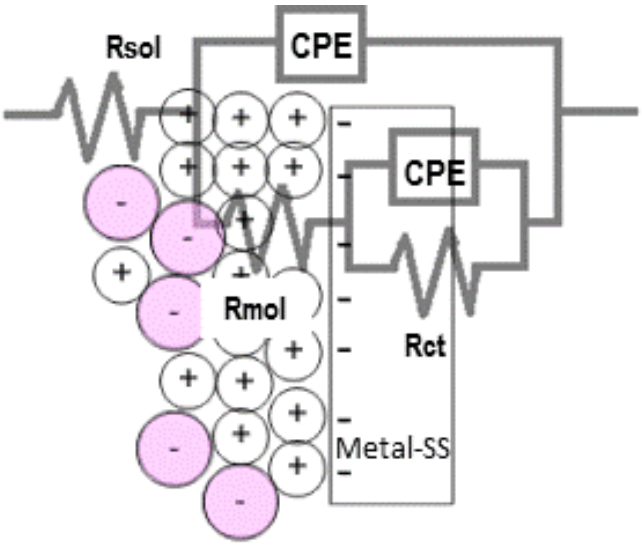

Figure 8. Electrical circuit equivalent model used to describe the experimental EIS diagrams: R_s solution resistance, CPE constant phase element, R_{mol} organic molecules resistance, and R_{ct} charger transfer resistance.

Table 3 shows the values of charge transfer resistance R_{ct} of impedance measurements, which shows that the maximum value of R_{ct} is achieved with a concentration of 40 ppm of BDI. These results are consistent with those obtained with the potentiodynamic tests presented in Table 2. Table 3 shows that the corrosion rate (*CR*) increases when the BDI concentration increases and decreases in BDI concentration range from 10 ppm to 40 ppm.

Table 3. EIS results obtained from 316L SS in 0.5M of H_2SO_4 with different concentrations of BDI, after 30 min of immersion in the mixture at 25°C.

Concentration ppm	R_s (Ωcm^2)	R_{mol} ($K\Omega cm^2$)	R_{ct} (Ωcm^2)	i_{corr} ($\mu A/cm^2$)	*CR* (mm/yr)	IE %
120	8.03	28456	62079	0.419	0.004794	30.0%
100	9.40	44680	95350	0.273	0.003121	54.4%
80	9.30	56843	113060	0.230	0.002632	61.5%
60	9.20	79800	122150	0.213	0.002437	64.4%
40	8.79	84546	255650	0.102	0.001164	83.0%
20	10.00	29699	86360	0.301	0.003446	49.7%

10	9.05	13054	51256	0.507	0.005807	15.2%
Blank	12.04	21620	43474	-	-	-

These results coincide with those proposed by Abdallah [23], Al-Mayouf [26], Oncul [22] and Hamza [27] who reported that compounds containing nitrogen in its structure are good corrosion inhibitors in different types of stainless steels in H_2SO_4, besides; their inhibitor efficiency is greater than 60%. The inhibition effect of these compounds is attributable to adsorption on the steel surface by means of the heteroatoms of active groups contained in the compound structure. Adsorption of BDI molecules on the stainless steel surface may be caused by fixing the two atoms of nitrogen over the empty orbitals "d" of the Fe atoms of the metallic substrate, inducing the formation of a protective film. This protective film could block the active anodic sites and limit the transport of H^+ ions or O_2 molecules on the metal surface, which interferes with the electrochemical reactions involved in the corrosion processes [40,41,42].

4. CONCLUSIONS

BDI becomes a good alternative to be used as a corrosion inhibitor for 316L SS in 0.5 M H_2SO_4 solution. The best behavior of the inhibitor was obtained at concentration of 40 ppm, values above or below these concentrations decreases the inhibitor efficiency due to the geometrical structure. Importantly, at a low concentration of the inhibitor (40 ppm at 25 °C), it is obtained a good inhibitor efficiency (75% approx.), this results indicate the viability of the inhibitor to be used in the pickling process of stainless steel. The inhibitor shows an anodic behavior as the potential is shifted to more positive values and the current density is shifted to lower values. The corrosion rate reduction may be due to the formation of a protective film of the inhibitor on the metal surface. The results derived from the polarization technique and electrochemical impedance were concordant. These electrochemical techniques allowed the determination of the behavior and efficiency of the BDI compound.

ACKNOWLEDGEMENT
The authors express their gratitude to Eng. María Estela Nuñez Pastrana, in the technical assistance during the synthesis of the inhibitor. The authors wish also to express their gratitude to the Mexican Institute of Transport, for Vehicular Engineering and Structural Integrity Coordination, Materials Laboratory, for its economic support to perform all the electrochemical tests in its facilities. HHH distinguishes to CONACyT for its research distinction as SNI1 and the stipend received monthly.

References

1. X.Y. Wang, Y.S. Wu, L. Zhang and Z.Y. Yu, *Corros. Sci., 57 (2001) 540.*
2. Y. Ait Albrimi, A. Eddib, J. Douch, Y. Berghoute, M. Hamdani and R.M. Souto, *Int. J. Electrochem. Sci*., 6 (2011) 4614.
3. R. Reinoza, *Cienc. Ing.*, 22 (2001) 33.
4. A.S. Fouda and A.S. Ellithy,*Corros. Sci.*,51 (2009) 868.
5. N.J. Sanders, *Anti-Corros Method. M. ,* 44 (1997) 20.
6. L. F. Li and J.P. Celis, *Can Metall Quart*,42 (2003), 365.
7. L.F. Lian, P. Caenen and J.P. Celis, *J. Electrochem Soc*, 152 (2005) B358.
8. W. Homjabok, S. Permpoon and G. Lothongkum, *J. Met MatMin s*, 20(2010)1.

9. ASTM Standard G15 *Standard Terminology Relating to Corrosion and Corrosion Testing*, United States (2004).
10. R.W. Revie and H.H. Uhlig, *Corrosion and corrosion control*, Wiley, Estados Unidos (2008).
11. L. Zamudio, A. Estrada and A. Benavides, *J. Mex. Chem. Soc., 46 (2002) 335.*
12. R. Herle, P. Shetty, S.D. Shetty and U.A. Kini, *Port. Electrochim. Acta* 29 (2011) 69.
13. S.A.Abd El–Maksoud, *Int. J. Electrochem. Sci*., 3 (2008) 528.
14. R. T. Loto, C. A. Loto, A. P.I. Popoola and M. Ranyaoa, *Int. J. Phys. Sci*., 7 (2012) 2136.
15. N. S. Patel, D. K. Patel, P. Kumari and G. N. Mehta, *Adv. in Nat. Appl. Sci.*, 3 (2009) 419.
16. N.F. Atta, A.M. Fekry and H.M. Hassaneen, *Int. J. Hydrogen Energ.*, 36 (2011) 6462.
17. N.A. Abdel, A.E.El-Shenawy and W.A.M. Hussien, *Mod. Appl. Sci*., 5 (2011) 19.
18. M. Scendo and J. Trela, *Int. J. Electrochem. Sci*., 8 (2013) 11951.
19. J. Aljourani, K. Raeissi, M.A. Golozar, *Corros. Sci.*, 51(2009) 1836.
20. Z, Zhang, S. Chen, Y. Li, S. Li and L. Wang, *Corros. Sci.*, (2009) 291.
21. R. Álvarez-Bustamante, G. Negrón-Silva, M. Abreu-Quijano, H. Herrera-Hernández, M. Romero-Romo, A. Cuán, M. Palomar-Pardavé, *Electrochem. Acta* 54 (2009) 5393.
22. A. Oncul, K. Coban and E. Sezer, *Prog. Org. Coat*., 71 (2011) 167.
23. M. Abdallah, Mat. *Chem. Phys*., 82 (2003) 786.
24. S.A.M. Refaey, F. Taha and A.M. Abd, El-Malak, *Int. J. Electrochem Sci*, 1(2006)80.
25. A.K. Satpati, P.V. Ravindran, *Mater Chem Physics*, 109(2008)352.
26. A. M. Al-Mayouf, A.K. Al-Ameery, and A.A. Al-Suhybani, *Corros. Sci*., 57 (2001) 614.
27. M.M. Hamza, S.S. Abd El Rehim and M. A.M. Ibrahim, *Arab. J. Chem*., 10 (2011)1016.
28. D.N. Morín, Actividad antimicrobiana de compuestos de coordinación de Metal (II)-Bencidiimidazol, M en C Thesis, Universidad Autónoma de San Luis Potosí (México) (2012).
29. ASTM Standard G3 Standard Practice for Conventions Applicable to Electrochemical Measurements in Corrosion Testing, United States (2004).
30. ASTM Standard G5 Standard Reference Test Method for Making Potentiostatic and Potentiodynamic Anodic Polarization Measurements, United States (2004).
31. ASTM Standard G 59 Standard Test Method for Conducting Potentiodynamic Polarization Resistance Measurements, United States (2003).
32. ASTM Standard G 106 Standard Practice for Verification of Algorithm and Equipment for Electrochemical Impedance Measurements, United States (2004).
33. K.F. Khaled, *Electrochim Acta*, 48 (2003) 2493.
34. S. Niketan, J. Smita, N. Girishkumar, *Chem. Pap*., 64 (2010) 51.
35. ASTM Standard G102 Standard practice for calculation of corrosion rates and related information from electrochemical measurements, United States (1999).
36. ASTM Standard G1 Standard Practice for preparing, cleaning, and evaluating corrosion test specimens, United States (2003).
37. C. Nathan, Corrosión Inhibitors, *Betz Laboratories Inc*., Houston (1981).
38. J. A. González , Control de la Corrosión: Estudio y Medida por Técnicas Electroquímicas, CSIC, Madrid (1989).
39. E. Sayed and M. Sherif, *Appl Surf Sci*, 292(2014)190.
40. A.G. Reynaud, M. Casales, J.G. Chacón, L. Martínez, A. Martínez y J.G. González, *FI. UNAM*, 10 (2009) 363.
41. S.A.M. Refaey et al, *Appl Surf Sci*, 236(2004)175.
42. R. Agrawal, T.K.G. Namboodhiri, *J Appl Electrochemistry*, 22 (1992)383.